Journal of Microscopy, Vol. 195, Pt 2, August 1999, pp. 96–103.
Received 8 June 1998; accepted 11 March 1999

Stereological estimation of covariance using linear dipole probes

M. G. REED & C. V. HOWARD
Fetal & Infant Toxico-Pathology, University of Liverpool, PO Box 147, Liverpool, L69 3BX, U.K.

Key words. Covariance, design based estimation, dipole probes, pair correlation function, second-order, spatial arrangement, vertical section, volume.

Summary

Classical stereology is capable of quantifying the total amount or 'density' of a geometrical feature from sampled information, but gives no information about the local spatial arrangement of the feature. However, stereological methods also exist for quantifying the 'local' spatial architecture of a 3D microstructure from sampled information. These methods are capable of quantifying, in a statistical manner, the spatial interaction in a structure over a range of distances. One of the key quantities used in a second-order analysis of a volumetric feature is the set covariance. Previous applications of covariance analysis have been 'model-based' and relied upon computerized image analysis. In this paper we describe a new 'design-based' manual method, known as linear dipole probes, that is suitable for estimating covariance from microscopic images. The approach is illustrated in practice on vertically sectioned lung tissue. We find that only relatively sparse sampling per animal is required to obtain estimates of covariance that have low inter-animal variability.

1. Introduction

Classical stereology is concerned primarily either with estimates of global quantities (volume, surface area, length, connectivity and number or their densities) or average quantities per particle (mean cell volume, mean surface area, etc.). However, stereological methods also exist for quantifying the 'local' spatial architecture of a 3D microstructure from sampled information (e.g. Cruz-Orive, 1989; Mattfeldt *et al.*, 1993, 1996). These methods are capable of assessing the degree of positive or negative correlation of a feature over a range of distances. Practical applications include the analysis of the spatial arrangements of osteocyte lacunae in skulls (Baddeley *et al.*, 1987, 1993), neurones and glial cells in human neo-cortex (Evans & Gundersen, 1989), cells and their DNA content (König *et al.*, 1991), the epithelial component of breast tumour tissue (Mattfeldt *et al.*, 1993), the orientation of glass fibres in composite materials (Mattfeldt *et al.*, 1994), the spatial distribution of pores in alumina (Karlsson & Liljeborg, 1994) and vertices in liquid foam (Reed *et al.*, 1997). Recent theoretical work in this area has been carried out by Cruz-Orive (1989), Jensen *et al.* (1990a,b), Jensen & Kiêu (1992) and Kiêu & Jensen (1993).

In this paper we focus on stereological methods suitable for quantifying the spatial architecture of a volumetric feature. The primary function used in this type of analysis is the covariance. Although the covariance is well known as a basic technique of quantitative image analysis (Serra, 1982; Gerlach & Stoyan 1986; Stoyan *et al.*, 1995) it is also well known in the statistical physics literature, where it is referred to as the two-point probability function (for example, see Torquato, 1998 and references therein). If the volume fraction, V_V, of the feature is also estimated then statistical functions derived from the covariance can be estimated, in particular the pair correlation function $g(r)$, see Mattfeldt *et al.* (1993).

Many published accounts of the estimation of covariance have adopted a 'model-based' approach in which the structure of interest has been assumed to be an isotropic random set and fixed sampling probes are used. In this paper we consider the 'design-based' case where the phase of interest is assumed to be non-random and randomised probes are used in estimation. In order to illustrate the approach we describe a simple manual method for estimation of covariance from vertical sampling designs and give a worked example of the method on vertically sectioned lung tissue.

2. First- and second-order stereology for volumes

The volume fraction of a phase, Y, within a bounded 3D reference space (i.e. an object) is defined as the volume of

Correspondence to: M. G. Reed,

the phase per unit volume of the reference space,

$$V_V(Y, ref) = \frac{\text{Volume of phase } Y \text{ in reference space}}{\text{Volume of reference space}}. \quad (1)$$

The notation $V_V(Y, ref)$ indicates volume fraction, with the parentheses specifying the phase of interest (e.g. Y) and the reference volume which is referred to. Volume fraction is a globally defined quantity ranging from 0 to 1 and on its own gives no indication of the spatial arrangement of the phase Y within the reference space.

Stereological estimation of volume fraction on cross-sections is carried out using area probes (Delesse, 1847), line grids (Rosiwal, 1898) or point grids (Thompson, 1930). However, in practice, quadratic point grids are the most commonly used method. Uniform random sections are sampled from the object and on uniform random fields of view a regular point grid is superposed. The number of points hitting the phase of interest, $P(Y)$, divided by the number hitting the reference space, $P(ref)$, gives a ratio-unbiased estimate of volume fraction,

$$\hat{V}_V(Y, ref) = P_P(Y, ref) = \frac{P(Y)}{P(ref)}. \quad (2)$$

Volume fraction estimation with point grids does not require either the magnification or interpoint spacing of the grid at the level of the micrograph to be known. The volume fraction of a phase is usually interpreted simply as a volumetric proportion; however, it can also be considered as a conditional hitting probability, $\Pr\{x \in Y \,|\, x \in ref\}$, i.e. the probability that a uniform random point x that hits the reference space will also land within the phase Y. This interpretation is closely linked to that of covariance, as defined below.

In volume fraction estimation only the total numbers of points hitting the phase Y and the reference space are recorded. However, intuitively one would expect that the pattern of points hitting Y would also give some information about the spatial arrangement of Y in 3D space. This is indeed the case if the number of pairs of points, separated by a particular distance, that hit Y on a section are recorded (e.g. Mattfeldt *et al.*, 1993; Stoyan *et al.*, 1995). Consider a straight line joining a pair of points a distance r units apart. The two end points of the line can be considered to be a single entity, which we refer to as a dipole, which 'hits' a particular phase Y if both of the endpoints land within the feature (note, however, that the line joining the two endpoints does not necessarily also need to be fully in Y; see Fig. 1a). The covariance of a volumetric feature Y, at a distance of r units, is defined as the conditional probability that an isotropic uniform random (IUR) dipole of length r units hits Y given that it has also hit the reference space i.e. $C(r) = \Pr\{x \in Y,\ x + r \in Y \,|\, x \in ref,\ x + r \in ref\}$. See Appendix for further details.

The covariance of a 3D phase Y, at a distance r, could be estimated by throwing a number of IUR dipoles of length r units into the reference space. The number of dipoles hitting the reference space $DP(ref,r)$ and the number hitting the phase Y, $DP(Y,r)$ are recorded and used to estimate covariance from

$$\hat{C}(r)_Y = \frac{DP(Y, r)}{DP(ref, r)}. \quad (3)$$

Although a range of dipoles of fixed length could be used (Fig. 1b.) to estimate covariance this would be inordinately time-consuming. In practice it is easier to use a regular point grid and record the positions of all points hitting phase Y. From these raw data a whole range of dipole lengths can be considered. For example, the pattern of point hits in a quadratic grid of interpoint spacing of 1 unit gives information about dipoles of length 1, $\sqrt{2}$, 2, ... , etc. (e.g. Mattfeldt *et al.*, 1993). Although quadratic and hexagonal grids have commonly been used a simple linear grid of points, or linear dipole probe, could be used.

Consider a line divided into m segments of equal length, Δ units, by a series of $n = m + 1$ points (Fig. 1c). If the line is superposed on a cross-sectional image a coded numerical record can be made for each of the points along the line indicating whether the point lands within the phase of interest Y (code = 1), within the reference space but outside Y, i.e. the 'background' (code = 2), or outside the reference space (code = 0). Each linear probe can thus yield dipole information at discrete radii of Δ, 2Δ, 3Δ, ... , $(n-1)\Delta$ units. These data can then be used to estimate covariance for $n-1$ discrete distances using Eq. (3).

It should be noted that the raw data used for covariance estimation can always be used to estimate volume fraction from Eq. (2), i.e. $\hat{V}_V = \hat{C}(0)_Y$. At a separation of zero units each 'dipole' will consist of a pair of points that are coincident in 3D space and thus Eq. (3) simplifies to Eq. (2). At longer distances the covariance tends to the reference value of ${V_V}^2$.

Practical stereological estimation of covariance with linear dipole probes requires that a number of IUR dipole probes can be generated. For example, IUR sections from isector (Nyengaard & Gundersen, 1992) or orientator (Mattfeldt *et al.*, 1990) sampling could be used, in which case the linear dipoles need to be isotropically rotated on the IUR plane section. More conveniently, IUR dipoles can also be generated on vertical uniform random (VUR) sections (Baddeley *et al.*, 1986). If VUR sections are used the vertical direction must be known and dipoles with a sine weighting with respect to the vertical must be used. Further practical aspects of the estimation procedure are outlined in section 3.

Although covariance gives a useful statistical description of spatial arrangement it is dependent upon volume fraction and, therefore, making comparisons between the covariance of two phases occupying different volume fractions can be problematic (see Mattfeldt *et al.*, 1993, for examples). The

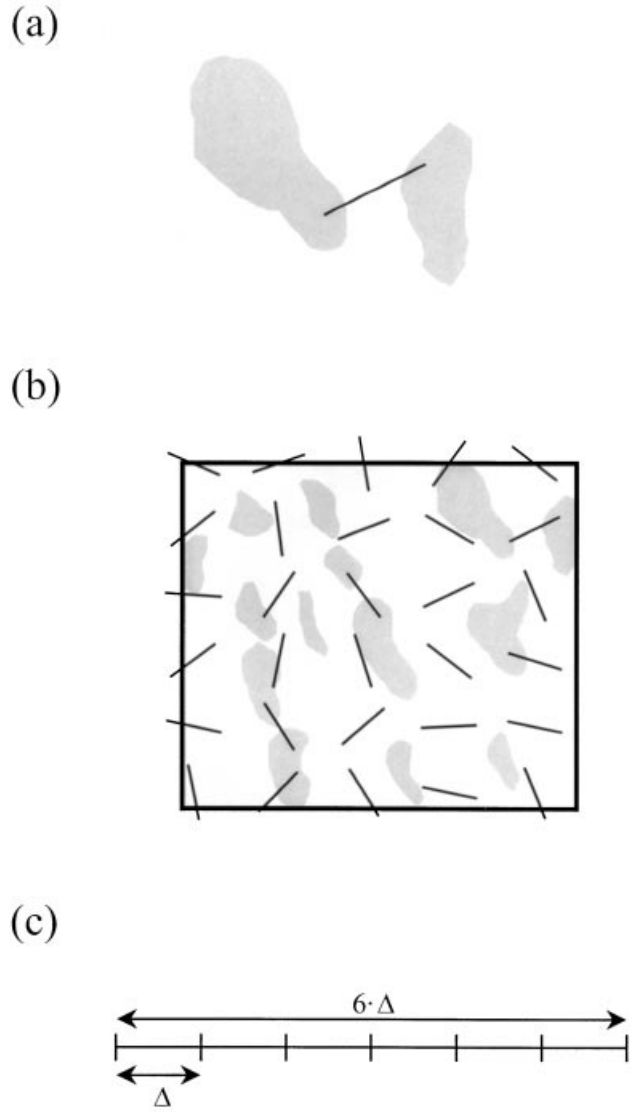

Fig. 1. (a) A schematic diagram illustrating the definition of a dipole 'hit'. Both ends of the dipole are considered to be a single entity and if both ends land within the phase of interest, in this case the grey feature, the dipole is said to hit that feature. It should be noted that the line joining the two test points does not have to lie fully within the phase of interest. (b) An example of covariance estimation for an isotropic uniform random field of view. A number of dipoles of fixed length with isotropic orientation within the plane have been randomly superposed on the field of view. The covariance of the darker grey feature at this distance is estimated from the number of dipoles hitting the phase (i.e. 3) divided by the number hitting the reference space within the field of view (i.e. 17), giving a covariance of 3/17. (c) A linear dipole probe composed of six segments of length Δ units.

dependence on volume fraction can be overcome by estimating the pair correlation function, $g(r)$, which is independent of volume fraction.

The pair correlation function is defined as the expected volume of the phase Y within a spherical shell of radii r and $r+dr$ which is centred at a statistically typical point of Y, divided by the expected volume of Y in a spherical shell of the same size centred at an arbitrary point in the structure;

$$g(r)_Y = \frac{E\,[\text{volume of } Y \text{ in spherical shell } (r, r+dr) \text{ centred at point of } Y]}{E\,[\text{volume of } Y \text{ in spherical shell } (r, r+dr) \text{ centred at arbitrary point of structure}]} \quad (4)$$

where $E[\cdot]$ indicates mathematical expectation.

The reference line for the pair correlation function is 1. Values of $g(r)$ greater (less) than unity indicate positive (negative) correlations of the volumetric feature. If estimates of covariance and volume fraction are available the pair correlation function can be estimated from

$$\hat{g}(r)_Y = \frac{\hat{C}(r)_Y}{\hat{V}_V(Y, ref)^2} \quad (5)$$

(see Mattfeldt *et al.* (1993)).

3. Worked example of the application of linear dipole probes

Four 7-day-old piglets from large white/landrace cross-bred sows were selected at random from a larger group of 16 animals, culled and immediately fixed in 10% neutral buffered formalin. The rapid fixing led to minor post-mortem changes in lung morphology and consequently technically excellent sections. The right lung from each piglet was removed and sagitally sectioned; the average slice thickness and cross-sectional areas estimated by point counting were used to estimate the volume of the lung by the Cavalieri method. Each of the lung sections were laid out flat and a transparent perspex template and metal punch were used to produce a set of systematic uniform random cylinders of tissue from each lung slice. These cylinders were processed and randomly rotated before vertically splitting into two half-cylinders, one of which was embedded in Historesin® (Leica, Milton Keynes, U.K.). Light microscopy sections of the embedded lung tissue 1 μm thick were prepared by microtome. These sections were then mounted on glass microscope slides and stained with 1% toluidine blue solution. The tissue vertical sections were observed with an Olympus BH-2 microscope using a 10× magnification 0·30 NA air objective. For each animal one field of view from each of five slides was recorded with a Sony XC-77E black and white CCD video camera and printed out as hardcopy.

For each image two sine-weighted directions were sampled using the grid from Cruz-Orive & Hunziker (1986). For each direction a set of four parallel linear dipoles was generated, with each dipole consisting of 20 points, separated by 35·7 μm at the level of the tissue. The pattern of points hitting the lung was encoded directly into

ASCII text files using a laptop PC. Points hitting alveolar airspace were recorded as a 1, points hitting bronchioles or other components of the lung matrix as a 2 and points landing outside the lung as a 0. An example of the use of the dipole probes on one of the vertical section images is shown in Fig. 2.

For each animal the ASCII files were analysed using a simple ANSI 'C' programme. The counts of dipoles within the alveolar airspace and reference space were pooled across all images within an individual before estimation of covariance. The point data from the ASCII files were also used to estimate the volume fraction of alveolar air space per unit volume of lung using Eq. (2). The estimated volume fraction and covariance for each animal were then substituted into Eq. (5) to give an estimated pair correlation function per animal. The mean pair correlation function across the four animals is plotted in Fig. 3, with 95% confidence intervals calculated using the standard deviation between the four animals and the Student's t distribution for three degrees of freedom.

The images from one of the animals were found to be of generally high contrast and were easy to segment. On these five images an image analysis estimation of covariance was carried out following the method described by Mattfeldt *et al.* (1993). In this analysis the 512×430 pixel images were segmented and every 10th pixel in the x and y directions sampled (giving a point grid of 51×43 pixels). The basic grid spacing of the quadratic array of 'hits' and 'misses' was $15{\cdot}7\,\mu$m at the level of the tissue. The pair correlation functions for this animal are shown in Fig. 4. The confidence intervals around the dipole probe estimated function were calculated with four degrees of freedom (i.e. between the five images).

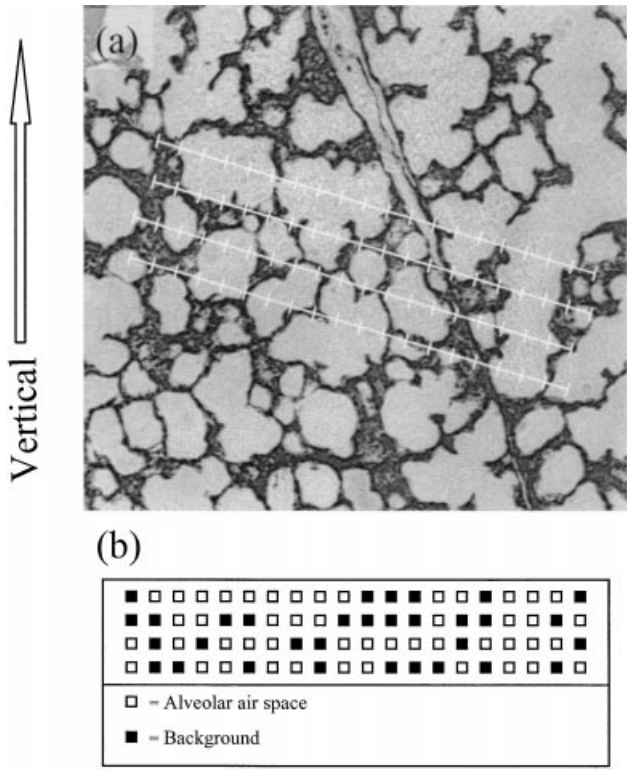

Fig. 2. (a) A vertical section of lung tissue from animal 11 with a sine-weighted set of four linear dipole probes. Each linear dipole probe consists of 20 points separated by $35{\cdot}7\,\mu$m at the level of the tissue. (b) The pattern of points hitting the alveolar airspace is shown as a series of white squares. Points hitting other parts of the lung matrix (bronchioles, blood vessels, etc.) are shown as black squares.

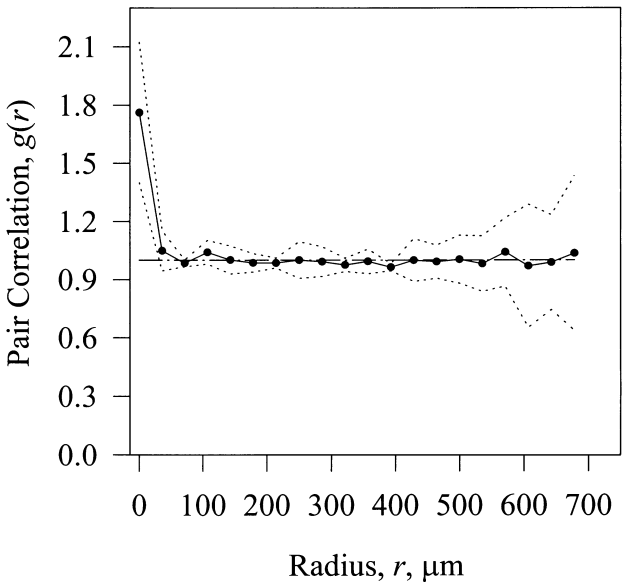

Fig. 3. A plot of the mean pair correlation function versus radius for the four animals (solid line with filled circles). In each case the pair correlation function was estimated using Eq. (5) from estimates of covariance and volume fraction made using Eqs (3) and (2), respectively. The pointwise 95% confidence intervals were calculated using the standard deviation between the four animals and the Student's t-distribution for three degrees of freedom (dotted lines). The increased variability of the estimates of pair correlation function with increasing distance is indicated by the wider confidence intervals at larger distances.

4. Discussion

Many of the methods used in stereology to quantify spatial arrangement have evolved from methods developed for the analysis of 2D point patterns found in ecology and geography (e.g. Getis & Boots, 1978; Ripley, 1981; Diggle, 1983; Cressie, 1993) and the analysis of 2D random sets (e.g. Serra, 1982). In many early applications of the 2D methods, replication was not considered and the single observed point or area pattern was assumed to be a realization (example) of a stochastic process. However, in

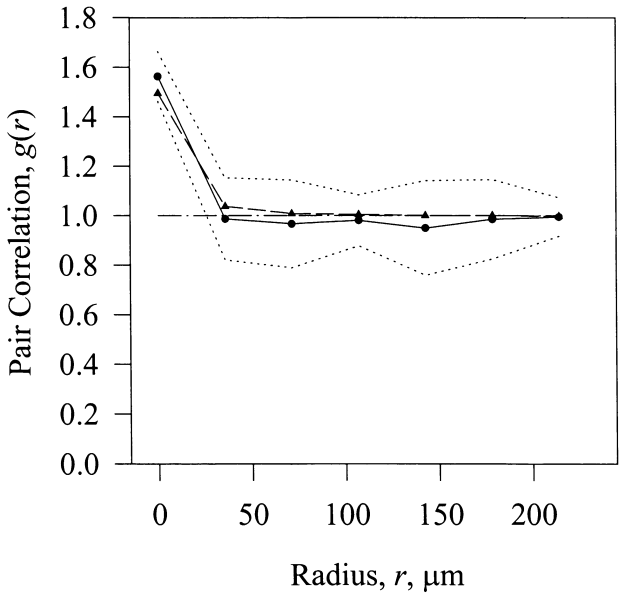

Fig. 4. A plot of the mean pair correlation function versus radius for one of the animals estimated using linear dipole probes (solid line with filled circles) and image analysis (dashed line with filled triangles). The pointwise 95% confidence intervals around the linear dipole estimates were calculated using the standard deviation between the five images and the Student's *t*-distribution for four degrees of freedom. The average coefficient of error between the five images over a range of radii 0–130 μm was found to be 21% for the image analysis and 25% for the linear dipole probe method.

many 3D problems where the quantification of the average spatial arrangement at a microstructural level is of interest there is the real possibility of taking many replicated samples of the pattern. If replicated samples of a spatial pattern are available the number and type of assumptions made in the analysis can be relaxed and also some measure of the variability of the spatial pattern can be made (e.g. Baddeley *et al.*, 1987, 1993).

The covariance estimation method described in this paper differs from previous methods by adopting a design-based sampling protocol. Design-based stereological methods are particularly useful for materials that cannot adequately be modelled as an isotropic random set. Many biological structures fall into this category; the objects are bounded in extent and often have highly ordered (i.e. non-random) internal microstructure. In these circumstances making the assumption that the structure is an isotropic random set may be inappropriate. Applying a design-based approach allows the investigator to apply covariance analysis to materials that are known not to be random. This may be particularly useful for materials that are heterogeneous but isotropic and for materials that have already been sectioned in an anisotropic manner, e.g. the vertically sectioned tissue used in this paper. It should be borne in mind that although the definition of covariance given here is independent of the anisotropy of the material being studied, in practice it would be of limited value to estimate the covariance of a strongly anisotropic material. If the material under study is known, or suspected to be, strongly anisotropic then the covariance could be plotted as a function of direction or a more appropriate measure of anisotropy used. Under these circumstances the analysis may well be easier with an image analyser.

In many histological applications the images that are obtained for stereological analysis are often of low and variable contrast and contain a great deal of information that is context specific. Under these circumstances the development of robust and reliable automatic segmentation is non-trivial and in many cases is unsolved. The inherent difficulty of analysing this type of image automatically has led to three broad methods of analysis. The first is to make an attempt at segmentation followed by manual image editing. The image editing can range from minor 'tidying up' of a segmented image to almost complete 'tracing' of the structures of interest using a mouse or digitizing tablet. The second approach is to use a hybrid method that uses computer graphics to generate suitable test grids and systems, followed by user input to mark intersection points, etc. The computer then uses this interactively generated data to calculate estimates of the required parameters. The hybrid approach thus makes a near optimal use of the relative strengths of both the computer and highly trained histologist. The computer is used to do what it is good at – accurate generation of interactive graphical elements of defined properties, recording of data, data handling and storage and numerical calculations. The expert is used to do what he/she is good at – making expert assessments of the detailed microstructure of a given piece of anatomy. The third approach is to use a fully manual method, using acetate overlays, manual recording of point counts, intercept lengths, etc, followed by numerical calculation. The optimal approach for a problem will be dictated to a large degree by the realities of the images that are generated, the degree of image analysis capability in a laboratory, cost of equipment, etc. In some cases automated image analysis will be a natural and obvious choice; in others the hybrid or manual approaches will be optimal.

If the images of interest can be reliably segmented into two phases then there are two well known image analysis techniques that can be applied. The classical image analysis technique developed at the Ecole des Mines, Fontainbleau, makes use of mathematical morphology. The covariance at a particular distance r is the volume fraction of the image eroded by a two-point structuring element separated by r (Serra, 1982). Some commercially available image analysis software systems can be programmed to automatically carry out this type of analysis. A related approach was described by Mattfeldt *et al.* (1993). In this method a

segmented image is subsampled by a quadratic grid of a given pixel spacing. The subsampling results in an array consisting of 1s, where the point grid hits the phase of interest, and 0s where the point grid hits the background. From the array of hits and misses the volume fraction and covariance can be easily calculated for a range of distances. The advantage of using digital image analysis for estimation of covariance is that the digitized and segmented images can readily be stored for future analysis.

In this paper we have concentrated on the estimation of covariance for situations where it is extremely difficult, or practically impossible, to segment the images. The estimation technique requires only the recording of the pattern of point hits generated by the use of a set of linear dipole probes on microscopic images or micrographs. Previous manual approaches for stereological estimation of the spatial architecture of a volumetric feature include the method proposed by Cruz-Orive (1989). However, this method required multiple distance measurements to be made and to the best of our knowledge has not been applied in practice. The estimation method described here can easily be taught, and in practice the recording of the pattern of 'hits' and 'misses' directly into ASCII files on a laptop PC whilst viewing the image with the linear dipole probes overlain is straightforward. Although the recording of point hits is more tedious than simple point counting it is possible to develop a very rapid recording technique. For example, the estimation of covariance for the lung tissue presented here took approximately 45 min per case; given that volume fraction estimation is obtained directly from the data that have been recorded for estimating the covariance the additional time taken for covariance estimation is therefore not excessive. A Microsoft® Windows®95 compatible program to estimate covariance from linear dipole data is available from the authors.

The linear dipole method is inherently less precise than image analysis methods which make use of all of the pixels making up an image. However, the precision of a stereological estimation technique is not simply dictated by the precision per 2D image. For example, in the case of vertical sections each of the 2D images used for analysis represents only a single orientation from the 2π radians possible for each position of the image plane. In this paper we compared the linear dipole method vs. image analysis for a single animal (Fig. 4). In order to get a rough idea of the relative components of the inherent between-image variability of covariance and that introduced by the linear dipole method we calculated the average coefficient of error (CE = standard error/mean) over the five images for the first four radii evaluated in the linear dipole method. The average CE for the image analysis method was found to be 21% and that for the dipole method 25%. If we assume that there is negligible error in estimation of 2D covariance using image analysis the 21% CE for the image analysis technique thus represents the inherent between-image variability; in other words, the lack of precision caused by sampling a 3D structure with 2D planes. Thus, although the image analysis method was found to be more precise than the dipole method, the bulk of the variability within a given animal was actually inherent between-image variability, and the increased variability introduced by the dipole sampling was relatively unimportant.

The use of both quadratic point grids and linear dipoles for covariance estimation has the attractive property that the estimates are automatically corrected for edge effect bias (see Stoyan *et al.*, 1995). This means that inter-feature distances that are an appreciable proportion of the size of the field of view can be considered. For example, in the lung tissue the covariance for inter-feature distances up to about 680 μm was estimated from images of width about 800 μm. In common with other spatial statistical methods, the precision of the covariance estimates decreases with increasing distance owing to the reduced number of point pairs hitting the reference space. For example, in animal 11, at a distance of 35·7 μm there were 800 dipoles landing within the reference space, of which 384 hit the alveolar airspace compared with 40 and 8 dipoles, respectively, for a distance of 678 μm. The increased variability at larger distances is reflected in the wider confidence intervals between animals shown in Fig. 3.

Potentially one of the most interesting aspects of the use of second-order stereology in biological applications is the small inter-animal variability of the estimated functions. This was first noted by Baddeley *et al.* (1987, 1993) in their analysis of the spatial distribution of osteocyte lacunae, but was also a notable feature of the analysis of mammary cancers by Mattfeldt *et al.* (1993) and recent work we have carried out on placental tissue (Reed, Howard, McFadden *et al.* unpublished results). A similar finding is also apparent here; the pair correlation function of alveolar airspace in lung has a smaller inter-animal variability across the four animals than the corresponding inter-animal variability of total alveolar volume. For example, for small inter-point distances the coefficient of error (CE) of the covariance estimates between the four animals was found to be about 3%, compared with a CE of alveolar volume estimates of 16%. The fact that local spatial architecture seems to be more invariant between animals than the total amount, or density, of a feature suggests that in a highly ordered biological microstructure second-order stereology may become increasingly important.

The results presented here indicate that the volume of the alveolar air space is highly positively correlated with itself at small distances (corresponding to distances within a single alveolus) and has no marked positive or negative correlation with itself at larger distances. Lung morphologists may say that this result is entirely expected. However, by applying a second-order analysis the possibility of quantifying this

previously qualitative understanding can be carried out with a relatively sparse sampling regime compared with either quadratic point grids (Mattfeldt *et al.*, 1993) or mathematical morphology (Serra, 1982). Our tentative conclusion is that if the average spatial architecture of a feature is required across a number of animals the well-known motto of first-order stereology, "Do more less well" (Gundersen & Østerby, 1981) may also be applicable. The combination of an efficiently estimated, meaningful and design-based measure of spatial architecture may make diagnostic second-order stereology a possibility.

Acknowledgements

We would like to thank Dr Darren Beech, Fetal & Infant Toxico-Pathology, University of Liverpool, for his kind permission to use the vertically sectioned lung tissue. We would also like to thank Professor Eva Vedel Jensen and an anonymous referee for valuable comments on an earlier version of the manuscript.

References

Baddeley, A.J. (1993) Stereology and survey sampling theory. *Bull. Intern. Statist. Inst., Proc. 49th Session, Florence, 1993*, **52** (2), 435–449.

Baddeley, A.J., Gundersen, H.J.G. & Cruz-Orive, L.M. (1986) Estimation of surface area from vertical sections. *J. Microsc.* **142**, 259–276.

Baddeley, A.J., Howard, C.V., Boyde, A. & Reid, S. (1987) Three-dimensional analysis of the spatial distribution of particles using the tandem-scanning reflected light microscope. *Acta Stereol.* **6** (Suppl. II), 87–100.

Baddeley, A.J., Moyeed, R.A., Howard, C.V. & Boyde, A. (1993) Analysis of a three-dimensional point pattern with replication. *Appl. Statist.* **42**, 641–668.

Cressie, N.A.C. (1993) *Statistics for Spatial Data* (2nd edn). Wiley, Chichester.

Cruz-Orive, L.M. (1989) Second-order stereology: estimation of second moment, measures. *Acta Stereol.* **8**, 641–646.

Cruz-Orive, L.M. & Hunziker, E.B. (1986) Stereology for anisotropic cells: application to growth cartilage. *J. Microsc.* **143**, 47–80.

Delesse, M.A. (1847) Procédé mécanique pour déterminer la composition des roches. *C.R. Acad. Sci. Paris.* **25**, 544–545.

Diggle, P.J. (1983) *Statistical Analysis of Spatial Point Patterns*. Academic Press, London.

Evans, S.M. & Gundersen, H.J.G. (1989) Estimation of spatial distributions using the nucleator. *Acta Stereol.* **8**, 395–400.

Gerlach, W. & Stoyan, D. (1986) Determination of the covariance of random sets from thin sections. *Biometr. J.* **4**, 427–432.

Getis, A. & Boots, B. (1978) *Models of Spatial Processes. An Approach to the Study of Points Lines and Area Patterns.* Cambridge University Press, Cambridge.

Gundersen, H.J.G. & Østerby, R. (1981) Optimizing sampling efficiency of stereological studies in biology: or 'Do more less well!'. *J. Microsc.* **121**, 65–73.

Jensen, E.B.V. & Kiêu, K. (1992) A note on recent research in second-order stereology. *Acta Stereol.* **11** (Suppl. I), 569–579.

Jensen, E.B., Kiêu, K. & Gundersen, H.J.G. (1990a) Second-order stereology. *Acta Stereol.* **9**, 15–35.

Jensen, E.B., Kiêu, K. & Gundersen, H.J.G. (1990b) On the stereological estimation of reduced moment measures. *Ann. Inst. Statist. Math.* **42**, 445–461.

Karlsson, L.M. & Liljeborg, A. (1994) Second-order stereology for pores in translucent alumina studied by confocal scanning laser microscopy. *J. Microsc.* **175**, 186–194.

Kiêu, K. & Jensen, E.B.V. (1993) Stereological estimation based on isotropic slices through fixed points. *J. Microsc.* **170**, 45–51.

König, D., Caravajal-Gonzales, S., Down, A.M., Vassy, J. & Rigaut, J.P. (1991) Modelling and analysis of 3-D arrangements of particles by point processes with examples of application to biological data obtained by confocal scanning light microscopy. *J. Microsc.* **161**, 405–433.

Mattfeldt, T., Clarke, A. & Archenhold, G. (1994) Estimation of the directional distribution of spatial fibre processes using stereology and confocal scanning laser microscopy. *J. Microsc.* **173**, 87–101.

Mattfeldt, T., Frey, H. & Rose, C. (1993) Second-order stereology of benign and malignant alterations of the human mammary gland. *J. Microsc.* **171**, 143–151.

Mattfeldt, T., Mall, G., Gharehbaghi, H. & Möller, P. (1990) Estimation of surface area and length with the orientator. *J. Microsc.* **159**, 301–317.

Mattfeldt, T., Schmidt, V., Reepschläger, D., Rose, C. & Frey, H. (1996). Centred contact density functions for the statistical analysis of random sets. *J. Microsc.* **183**, 158–169.

Miles, R.E. (1978) The importance of proper model specification in stereology. *Geometrical Probability and Biological Structures: Buffons's 200th Anniversary. Lecture Notes in Biomathematics 23* (ed. by R. E. Miles and J. Serra), pp. 115–136. Springer-Verlag, Berlin.

Nyengaard, J.R. & Gundersen, H.J.G. (1992) The isector: a simple and direct method for generating isotropic, uniform random sections from small specimens. *J. Microsc.* **165**, 427–431.

Reed, M.G., Howard, C.V. & Shelton, C.G. (1997) Confocal imaging and second-order stereological analysis of a liquid foam. *J. Microsc.* **185**, 313–320.

Ripley, B.D. (1981) *Spatial Statistics*. Wiley, New York.

Rosiwal, A. (1898) Ueber geometrische Gesteinsanalysen. *Verh. K.K. Geol. Reichsant. Wien.* **54**, 11. (Cited in Weibel, E.R. (1979) *Stereological Methods. Vol 1: Practical Methods for Biological Morphometry.* Academic Press, London.)

Serra, J. (1982) *Image Analysis and Mathematical Morphology.* Academic Press, London.

Stoyan, D., Kendall, W.S. & Mecke, J. (1995) *Stochastic Geometry and its Applications* (2nd edn). Wiley, Chichester.

Thompson, E. (1930) Quantitative microscopic analysis. *J. Geol.* **38**, 193.

Torquato, S. (1998) Morphology and effective properties of disordered heterogenous media. *Int. J. Solids Structures.* **35**, 2385.

Appendix – Design-based definition of covariance

The non-centred covariance of a set Y is defined as the probability that a pair of points x and $x+r$, separated by

distance of r units, both hit Y,

$$C(r) = \Pr\{x \in Y, x + r \in Y\}. \quad \text{(A1)}$$

This definition has usually been applied under the assumption that Y is a stationary random set (Serra, 1982; Mattfeldt *et al.*, 1993). However, with a small modification the same definition can be applied to the extended deterministic case described by Miles (1978). Consider a bounded and non-random set $X \subset R$, containing a distinct bounded and non-random subset $Y \subseteq X$ (not necessarily connected). The probability that a pair of points hits the phase Y must now take account of the possibility of pairs of points completely missing the reference space X. Under these constraints the covariance can be defined as a conditional probability, i.e.

$$C(r) = \Pr\{x \in Y, x + r \in Y | x \in X, x + r \in X\}. \quad \text{(A2)}$$

This function is clearly dependent upon the bounding set X. However, if X is assumed to be much larger than the range of distances of interest, the extended deterministic model of Miles (1978), Eq. (A2) has a similar interpretation as in the stationary case (Stoyan *et al.*, 1995).

In order to calculate the probability in Eq. (A2) an integration over all pairs of points of separation r units that hit the reference space needs to be made. Let $\mathbf{x}$ denote the Cartesian co-ordinate of a point in R^3, u an orientation vector on the unit orientation sphere S^2 and $\mathbf{h}(r,u)$ a vector of length r units and orientation u. The conditional probability in Eq. (A2) is given by

$$C(r)_Y = \frac{\int_{x \in X} \int_{u \in S} \mathbf{1}(\mathbf{x} \in Y) \cdot \mathbf{1}(\mathbf{x} + \mathbf{h}(r,u) \in Y) d\mathbf{x} du}{\int_{\mathbf{x} \in X} \int_{u \in S} \mathbf{1}(\mathbf{x} \in X) \cdot \mathbf{1}(\mathbf{x} + \mathbf{h}(r,u) \in X) d\mathbf{x} du}. \quad \text{(A3)}$$

where $\mathbf{1}(.)$ is the indicator function, defined as 1 if true and 0 otherwise. This definition of covariance is thus equal to the probability that both $\boldsymbol{x}$ and $x + \mathbf{h}(r,u)$ will hit Y conditional on the fact that they both hit the set X.

The ratio defined by Eq. (A3) can be estimated by sampling a number, n, of uniform random (UR) points $\mathbf{x}_i$ over X. For each of these points a uniform random orientation is sampled from the unit orientation sphere (i.e. an isotropic direction), thus defining a point pair $\mathbf{x}_i$ and $\mathbf{x}_i + \mathbf{h}(u,r)_i$. A 'ratio-unbiased' estimate (Baddeley, 1993) of Eq. (A3) is then obtained from

$$\hat{C}(r)_Y = \frac{\sum_{i=1}^{n} \mathbf{1}(\mathbf{x}_i \in Y) \cdot \mathbf{1}(\mathbf{x}_i + \mathbf{h}(u,r)_i \in Y)}{\sum_{i=1}^{n} \mathbf{1}(\mathbf{x}_i \in X) \cdot \mathbf{1}(\mathbf{x}_i + \mathbf{h}(u,r)_i \in X)}. \quad \text{(A4)}$$

where $\mathbf{x}_i$ and $\mathbf{h}_i$ are the ith point and orientation, respectively. It should be noted that a point pair $\mathbf{x}_i$ and $\mathbf{x}_i + \mathbf{h}(u,r)_i$ contributes to the numerator or denominator of Eq. (A4) if and only if both points land within the set of interest (Y and X, respectively); then Eq. (3) is a simple restatement of (A4). In practice, the generation of UR points and isotropic lines can be carried out on either IUR or VUR sections.

In common with the model-based definition of covariance the value of $C(r)$ for $r = 0$ is simply the volume fraction V_V. However, it should be noted that in distinction to the model-based definition the covariance given by Eq. (A3) at infinity is zero not ${V_V}^2$. In many practical cases the object X will be much larger than the maximum radius of interest, r_{max}, in which case $C(r >> r_{max}) \approx {V_V}^2$.